Available online at www.sciencedirect.com
SCIENCE DIRECT®
Planetary and Space Science 53 (2005) 299–305
Planetary and Space Science
www.elsevier.com/locate/pss

Central position of the source region of storm-time chorus

O. Santolík[a,*], D.A. Gurnett[b], J.S. Pickett[b], M. Parrot[c], N. Cornilleau-Wehrlin[d]

[a]Faculty of Mathematics and Physics, Charles University, V Holesovickach 2, 180 00 Prague, Czech Republic
[b]Department of Physics and Astronomy, University of Iowa, Iowa City, USA
[c]Laboratoire de Physique et Chimie de l'Environnement, CNRS, Orléans, France
[d]Centre d'étude des Environnements Terrestre et Planétaires, IPSL/CNRS, Vélizy, France

Accepted 12 September 2004

Abstract

We describe an analysis method to estimate the central position of the source region of electromagnetic waves. The method is based on simultaneous measurements of the Poynting flux in several points in space. We analyze measurements of whistler-mode chorus by the four spacecraft of the Cluster mission close to their perigee at a radial distance of 4 Earth radii. The data were recorded on the nightside during disturbed periods on 31 March 2001 and 18 April 2002. The derived central position of the chorus source region is close to the geomagnetic equator, as it has been shown by previous studies. This global centrum of the source region is defined by the equilibrium of the Poynting flux parallel and antiparallel to the field line. The central position is found to randomly move back and forth with an amplitude of a few thousands of kilometers on time scales of minutes. The typical order of magnitude of the speed of this motion is 100 km/s. We exclude the possibility of flapping of a tail-like configuration of the ambient magnetic field. These random fluctuations of the central position of the source region are thus connected to the generation mechanism itself.

Keywords: Whistler-mode chorus; Poynting flux measurements; Cluster project; STAFF spectrum analyzer; WBD receiver

1. Introduction

Emissions of chorus are electromagnetic waves propagating in the whistler mode in the inner magnetosphere. They typically have a discrete structure of separate wave packets in a frequency range from a few hundreds of Hertz to several kilohertz (see reviews by Omura et al., 1991; Sazhin and Hayakawa, 1992, and references therein). Chorus is generated by nonlinear interactions involving the electron cyclotron resonance of whistler-mode waves with energetic electrons (e.g., Helliwell, 1967; Tsurutani and Smith, 1974; Nunn et al., 1997; Trakhtengerts, 1999). Intense chorus generated during geomagnetic storms can accelerate energetic electrons in the outer radiation belt (e.g., Meredith et al., 2003; Horne and Thorne, 2003) and is thus an important element in understanding the physical processes occurring during the disturbed times.

The region of interest for recent investigation of chorus has been its source (Lauben et al., 1998; LeDocq et al., 1998; Gurnett et al., 2001; Parrot et al., 2003; Santolík and Gurnett, 2003; Santolík et al., 2003). The theory predicts that the source region, centered at the geomagnetic equator, has a characteristic dimension of a few thousands of kilometers in the direction parallel to the terrestrial magnetic field ($\boldsymbol{B}_0$) (Helliwell, 1967; Trakhtengerts, 1999), while a characteristic scale of a few hundreds of kilometer was predicted by Trakhtengerts (1999) for spatial features of chorus generation in the direction perpendicular to $\boldsymbol{B}_0$. Both these scales have been confirmed recently through observations of the Cluster spacecraft (Santolík and Gurnett, 2003; Santolík et al., 2003, 2004). The position of the source region has been investigated using the Poynting flux measurements on board the Polar and Cluster spacecraft (LeDocq et al., 1998; Parrot et al., 2003; Santolík et al., 2003). The measurements have shown that

*Corresponding author. Tel.: +420 2 2191 2302; fax: +420 2 688 5095.
E-mail address: ondrej.santolik@mff.cuni.cz (O. Santolík).

0032-0633/$ - see front matter © 2004 Elsevier Ltd. All rights reserved.
doi:10.1016/j.pss.2004.09.056

the Poynting vector always had a component parallel to $\boldsymbol{B}_0$ if the spacecraft was to the North of the geomagnetic equator, and antiparallel to $\boldsymbol{B}_0$ when the measurements were carried out on the southward side of the equator. In the frequency range where chorus is observed, anisotropic propagation properties of the whistler-mode waves imply that the component along $\boldsymbol{B}_0$ is always the largest component of the Poynting vector. The observed change of the sign of this component thus indicates a positive divergence of the Poynting flux and therefore the presence of the source region of chorus.

In the present paper, the central position of the chorus source region will be defined as the point where the parallel component (with respect to $\boldsymbol{B}_0$) of the Poynting flux changes its sign. LeDocq et al. (1998) and Parrot et al. (2003) have found this position close to the geomagnetic equatorial plane or to the place where the magnetic field is minimum along a given field line (minimum-B equator). We present a method of investigation of the motion of the central position using simultaneous measurements at several points in space. The first results of that method were briefly presented as a part of the analysis of storm-time chorus on 31 March 2001 (Santolík et al., 2004). In the present paper, we describe the method in detail, we show similar results for another storm-time case, and we discuss the influence of the configuration of the ambient magnetospheric magnetic field on the results. In Section 2 we describe the measurements and the data processing methods. The method of estimation of the central position of the source region is then presented in Section 3 using two storm-time cases. Finally, in Sections 4 and 5 we discuss and briefly summarize the results.

2. The data and processing methods

The analysis is based on simultaneous measurement of several instruments onboard the four Cluster spacecraft. Detailed time–frequency power spectrograms are obtained from measurements of the wideband (WBD) plasma wave receivers (Gurnett et al., 2001). These spectrograms allow us to verify the presence of the discrete structure of separate wave packets. The electron–cyclotron frequency and the direction of the ambient magnetic field are determined from measurements of the onboard flux-gate magnetometers (FGM) (Balogh et al., 2001). The Poynting flux data which are the most important for this study are derived from multicomponent measurements obtained by the spectrum analyzers of the "spatio-temporal analysis of field fluctuations" (STAFF) instruments (Cornilleau-Wehrlin et al., 2003). These instruments analyze signals of three magnetic and two electric antennas and calculate the auto-power spectra and cross-power spectra in 27 logarithmic frequency channels between 8 Hz and 4 kHz, with a time resolution between 1 and 4 s.

The auto-power spectra and cross-power spectra are, in each frequency channel, represented as 5×5 spectral matrices. These matrices are transformed to the coordinate system linked to the local direction of the ambient magnetic field obtained from the FGM data. Then, we average the spectral matrices over the frequency interval where chorus is observed, based on the detailed time–frequency spectrograms from the WBD instrument. Finally, we use Eq. (8) of Santolík et al. (2001) to obtain an estimate of the parallel component of the Poynting vector normalized by its standard deviation $S_{\parallel}/\sigma(S_{\parallel})$, where the normalization factor $\sigma(S_{\parallel})$ is estimated from errors induced by the spectral analysis.

3. Analysis of the central position of the chorus source

Fig. 1 shows an overview time–frequency power-spectrogram of the electric field fluctuations measured

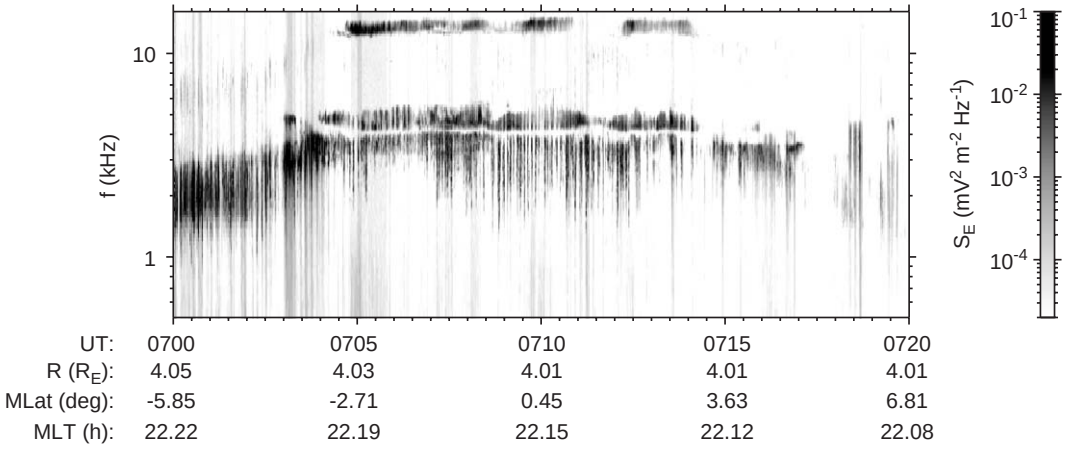

Fig. 1. Power-spectrogram of the electric field measured onboard Cluster 3 on 31 March 2001. Position of the spacecraft is given on the bottom. R—radial distance in Earth radii; MLat—magnetic dipole latitude in degrees; MLT—magnetic local time in hours.

by the WBD instrument onboard Cluster 3. The measurements were recorded under very disturbed conditions on 31 March 2001, when the K_p index reached the value of 9^- and the D_{st} index decreased to -358 nT. Baker et al. (2002) observed injection of substorm energetic electrons in the pre-midnight sector. In this sector we also observe intense whistler-mode chorus emissions in the frequency range 1–6 kHz. During the time interval shown in Fig. 1, the spacecraft was close to its perigee at ~ 4 Earth radii (R_E) and moved along its orbit through the equatorial region from the South to the North. The observed chorus emissions are organized into two bands, separated by a gap of decreased power, as reported previously by, e.g., Anderson and Maeda (1977). The upper band only appears close to the geomagnetic equator and its lower-frequency limit at ~ 4 kHz follows one-half of the local electron–cyclotron frequency (f_{ce}). Simultaneously we observe another band of intense emissions at frequencies above 12.5 kHz.

The lower band of chorus below $\frac{1}{2}f_{ce}$ extends in both hemispheres towards higher magnetic latitudes, decreasing in frequency. Below 4 kHz, this lower band is simultaneously observed by the STAFF instruments onboard the four Cluster spacecraft. Fig. 2 shows $S_\parallel/\sigma(S_\parallel)$ calculated in this frequency band from the data of each of the spacecraft. As we can expect, the parallel component of the Poynting flux turns from negative to positive values close to the times when the spacecraft cross the equatorial plane during their orbital motion. The transition from negative to positive values is not smooth, though. On Cluster 1 and 3 the sign clearly switches several times during the transition interval.

Fig. 3 shows that these fluctuations can be well explained if we take into account the positions of the spacecraft. While their maximum separation in the equatorial plane was ~ 370 km (Fig. 3b), the maximum separation was ~ 1600 km in the direction perpendicular to that plane. In Fig. 3a, the Z_{SM} coordinate (perpendicular to the magnetic equator) of the four spacecraft is represented as a function of time by four oblique lines extending from the lower left to the upper right corner of the figure. The widths of these lines reflect the values of $S_\parallel/\sigma(S_\parallel)$ after averaging to a time resolution of 25.5 s; the thin line corresponds to values lower than -1, while the thick line means values higher than $+1$. We can see that a clear boundary (dotted line in Fig. 3a) can be drawn, separating the positive and negative values of

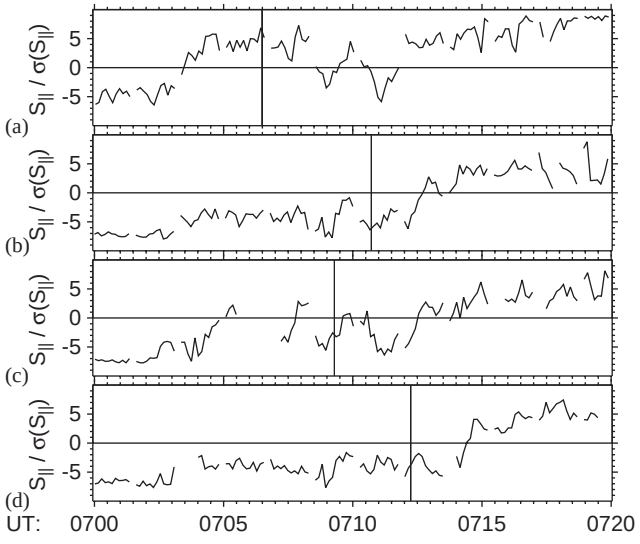

Fig. 2. Parallel component of the Poynting vector normalized by its standard deviation. Panels (a)–(d) show the results for Cluster 1–4, respectively. The vertical line in each panel indicates the time when the given spacecraft encounters the magnetic equatorial plane (zero magnetic latitude). A dipole model is used.

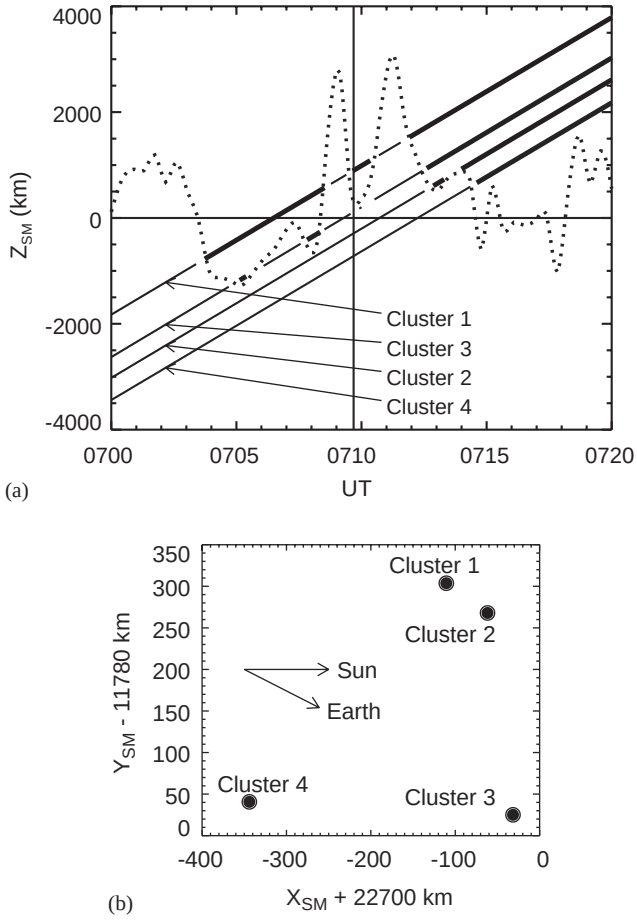

Fig. 3. (a) Four oblique lines represent changes of the sign of $S_\parallel/\sigma(S_\parallel)$ along the orbit of the four Cluster spacecraft with the Z_{SM} coordinate plotted as a function of time; the dotted line is the estimated central position of the chorus source region (see text). The horizontal solid line is the magnetic equator obtained from a dipole model, the vertical solid line shows the time when the center of mass of the four spacecraft crosses the equator. (b) Positions of the spacecraft in the equatorial plane. Arrows show the earthward and the sunward directions.

$S_\parallel/\sigma(S_\parallel)$ and hence indicating the central position of the chorus source region.

To estimate this central position at a given time we have used an approximation method based on linear interpolation or extrapolation of the obtained $S_\parallel/\sigma(S_\parallel)$ values. The procedure is as follows:

(1) We order the four spacecraft to obtain a growing sequence of their Z_{SM} coordinates.
(2) If $S_\parallel/\sigma(S_\parallel)$ has a different sign on two neighboring spacecraft in the sequence, we calculate the central position Z_0 using linear interpolation between the Z_{SM} coordinates of these two spacecraft,

$$Z_0 = Z_{SM(k)} - \frac{(S_\parallel/\sigma(S_\parallel))_{(k)}}{(S_\parallel/\sigma(S_\parallel))_{(k+1)} - (S_\parallel/\sigma(S_\parallel))_{(k)}} \times (Z_{SM(k+1)} - Z_{SM(k)}),$$

where the unique indices (k) and $(k+1)$ denote the two spacecraft, k ranging from 1 through 3.
(3) If the above condition (2) is not fulfilled, Z_0 is estimated using linear extrapolation from the Z_{SM} coordinate of the spacecraft m where $S_\parallel/\sigma(S_\parallel)$ is minimum,

$$Z_0 = Z_{SM(m)} - b(S_\parallel/\sigma(S_\parallel))_{(m)},$$

where m ranges from 1 through 4, and b is a coefficient described below.

Z_0 values obtained using this procedure are then plotted as a function of time in Fig. 3a (dotted line).

The coefficient b of the linear extrapolation (3) is obtained from a linear model $Z_{SM} = a + b \times S_\parallel/\sigma(S_\parallel)$ based on the data from the entire time interval shown in Fig. 2. The results from the different spacecraft are very similar and we thus combine the data from the four spacecraft. The obtained points and their linear model are presented in Fig. 4a. The parameters a and b and their standard deviations were obtained by a straightforward linear least-squares fit procedure. To check if the estimated coefficient b is stable, we have performed the same least squares fit for the differences of Z_{SM} and the estimated central position Z_0. Fig. 4b shows that the resulting coefficient b is nearly the same as in Fig. 4a.

On 31 March 2001 the measurements were recorded during the period when the Cluster spacecraft were at relatively large separations. The question thus may arise whether similar results can also be obtained when the spacecraft are at closer separations. Approximately 1 year later, on 18 April 2002, a geomagnetic storm hit the Earth's magnetosphere when the Cluster spacecraft were near their perigee at the maximum separation of ~ 260 km along $\boldsymbol{B}_0$ and ~ 100 km in the perpendicular plane (Santolík et al., 2003). During that storm, the D_{st} index decreased below −120 nT and the Kp index reached 7^0. Intense chorus emissions were again generated, and the obtained values of $S_\parallel/\sigma(S_\parallel)$ are

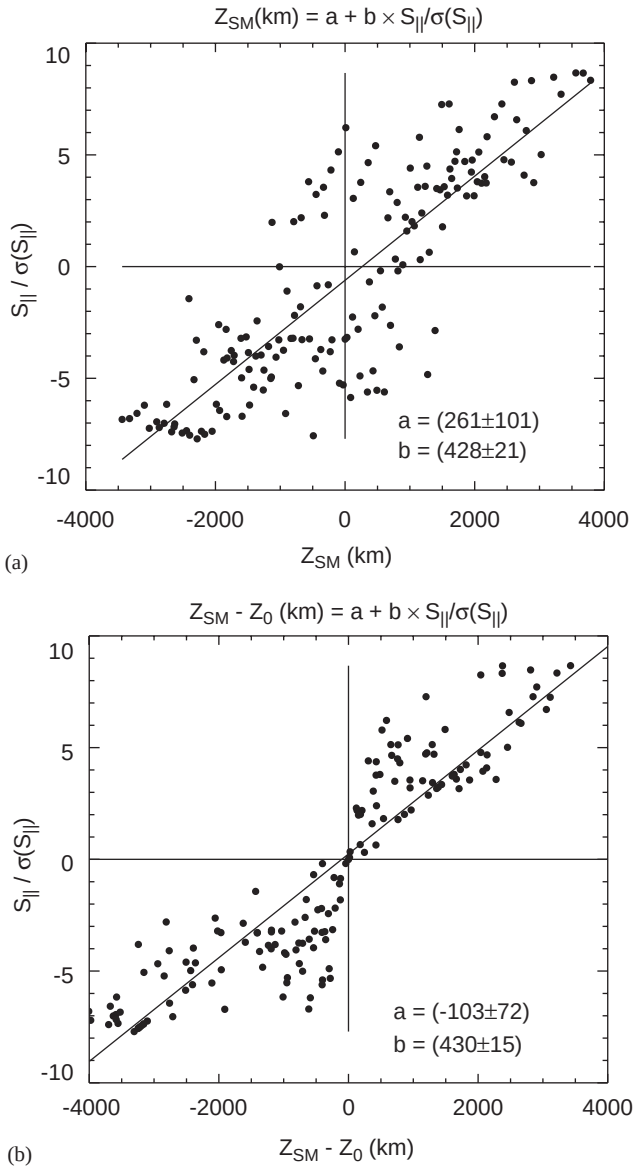

Fig. 4. (a) Linear fit to the obtained $S_\parallel/\sigma(S_\parallel)$ values as a function of the Z_{SM} coordinate. (b) The same but using the difference of the Z_{SM} coordinate and the estimated central position of the source.

shown in Fig. 5. As in the previous case, the transition from negative to positive values is not smooth. On the other hand, the fluctuations are now nearly the same on the four spacecraft. This is a consequence of their close separation along $\boldsymbol{B}_0$.

The Z_{SM} coordinates of the four spacecraft, together with the sign of $S_\parallel/\sigma(S_\parallel)$, are presented in Fig. 6. The data are averaged to the time resolution of 12.8 s. We have selected a time interval two times shorter than that in Fig. 3 because of much smaller differences in the Z_{SM} coordinates of the spacecraft. The central position of the source region is calculated by the same method as previously and shown by the dotted line. We can see that the results are similar as in the previous case, including the results for the linear model of $S_\parallel/\sigma(S_\parallel)$ as a function of Z_{SM} (Fig. 7).

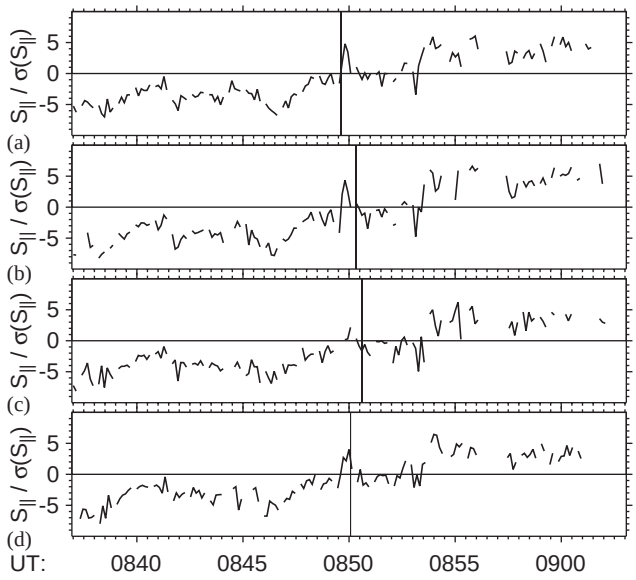

Fig. 5. Same as in Fig. 2 but for measurements recorded on 18 April 2002.

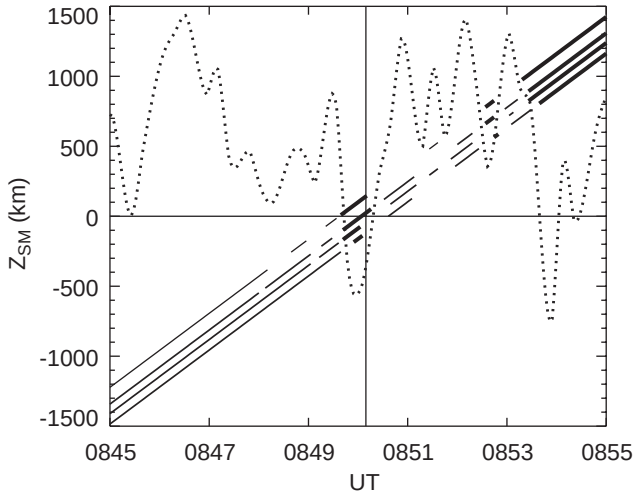

Fig. 6. Same as in Fig. 3 for measurements recorded on 18 April 2002.

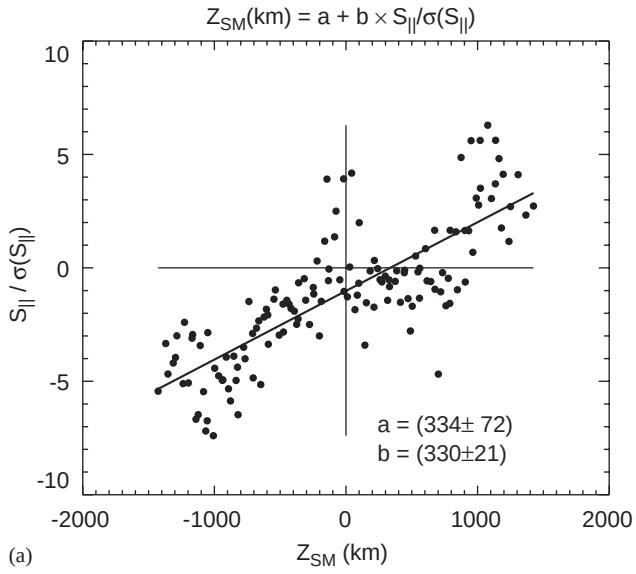

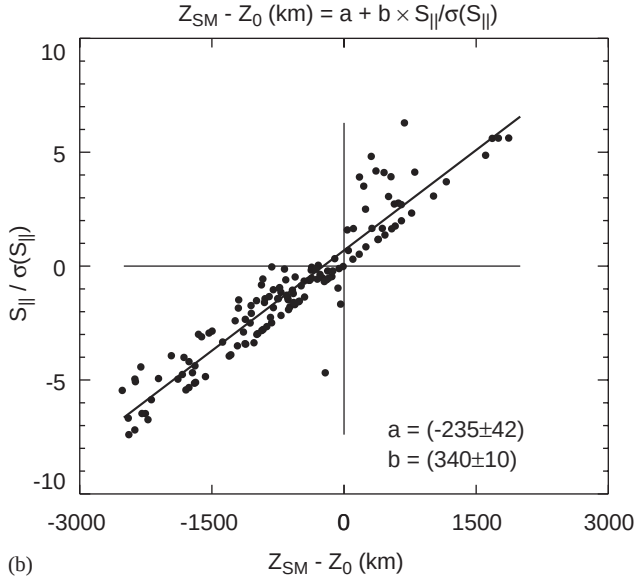

Fig. 7. The same as in Fig. 4 but for the data recorded on 18 April 2002.

4. Discussion

The analysis presented above allows us to estimate the location of the "central position" of the source region of whistler-mode chorus. It has to be noted that this position is not necessarily the geometric center of the source region. We define the "central position" as the point where the parallel component of the total Poynting flux changes its sign. We suppose that the source region has a finite dimension of a few thousands of kilometers along the field line (Santolík et al., 2004). Inside this source region both directions of the Poynting flux are present simultaneously but on its southern side, the waves propagating to the South prevail, and similarly on its northern side we mainly observe the waves propagating to the North. The central position of this source region is then the point inside the source region where the parallel Poynting flux of waves propagating into the northern hemisphere equals the parallel flux of the waves propagating to the southern hemisphere.

We have observed random fluctuations of the estimated central position of the source region. There are two possible explanations. Either this is a property of the source mechanism itself, or the entire magnetic configuration is tail-like and flaps over the spacecraft, carrying the chorus source region with it. Under quiet conditions this latter possibility is not very likely to happen at the radial distance of our observations ($\sim 4R_E$). However, during storm conditions it is not

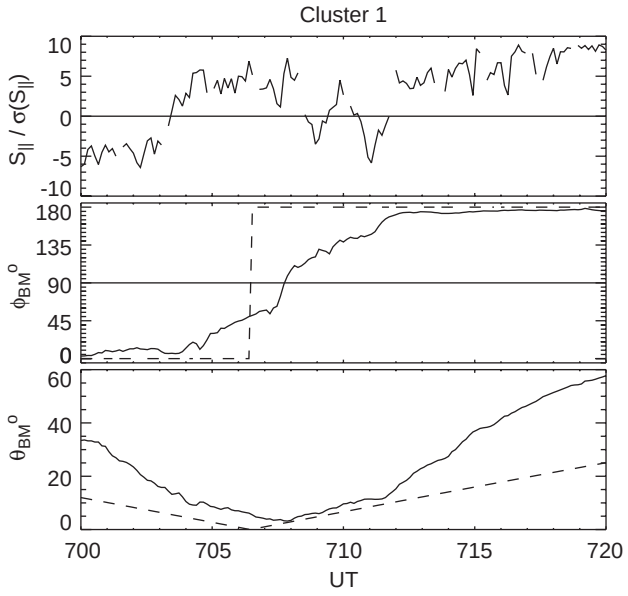

Fig. 8. Comparison of the normalized parallel component of the Poynting flux $S_\parallel/\sigma(S_\parallel)$ with the direction of the ambient magnetic field $\boldsymbol{B}_0$ expressed by azimuth $\phi_{\rm BM}$ measured around the $Z_{\rm SM}$ axis from the plane of the local meridian, and by the angle $\theta_{\rm BM}$ between the $\boldsymbol{B}_0$ direction and the $Z_{\rm SM}$ axis. Solid line corresponds to the onboard measurement, dashed line shows the dipole model.

unrealistic to have strong magnetic distortions at this radial distance. We have thus examined this possibility for the case of 31 March 2001. Fig. 8 shows $S_\parallel/\sigma(S_\parallel)$ measured onboard Cluster 1, together with the direction of the ambient magnetic field $\boldsymbol{B}_0$ measured on the same spacecraft, and with the simulated results obtained from the dipole model calculated along the spacecraft orbit. We can see that the deviation $\theta_{\rm BM}$ of the $\boldsymbol{B}_0$ direction from the $Z_{\rm SM}$ axis is larger than the dipole model predicts, corresponding to a tail-like configuration. However, no flapping is observed since the azimuth $\phi_{\rm BM}$ turns just once from the outward to the inward direction. The observed random fluctuations are thus associated with the source mechanism of the storm-time chorus emissions.

It is important to note that our method does not allow us to resolve the individual wave packets of chorus. In one single multicomponent measurement of the STAFF spectrum analyzer, we accumulate the data over almost 4 s, which means that we usually mix the information from several wave packets. We are thus unable to check the hypothesis of rapid motion of sources of individual wave packets (Inan et al., 2003), according to which the sources are moving at speeds comparable to the phase speed of the whistler-mode waves (of the order of 10^4–10^5 km/s). Our analysis can only provide global characteristics of the Poynting flux direction in the source region. The changes of this globally defined central position are found to happen on the time scale of minutes. This is not just an effect of the lower time resolution compared to the duration of individual wave packets: we often consistently observe the same sign of the parallel component of the Poynting flux in sequences of many data points, during time periods of the order of minutes. Combining this time scale with the amplitude of a few thousands of kilometers we obtain a global motion with typical speeds on the order of 100 km/s.

5. Conclusions

(1) A new multipoint analysis method to estimate the central position of the source region of electromagnetic waves has been proven to give useful results.
(2) We have analyzed storm-time chorus emissions recorded by the four spacecraft of the Cluster mission on 31 March 2001 and on 18 April 2002. We have obtained qualitatively similar results in both these cases, while the spacecraft separations were significantly different.
(3) The global central position of the source region has been shown to fluctuate within a few thousands of kilometers at a typical speed of the order of 100 km/s.
(4) This random motion is most probably associated with the generation mechanism of chorus.

Acknowledgements

We sincerely thank Chris Harvey, Milan Maksimovic, and other colleagues from the STAFF team for construction, calibration and operations of the instrument and for fruitful discussions of the data. Our thanks are due to the PI of the FGM instrument (A. Balogh) for the DC magnetic field data, and to the Hungarian Cluster Data Center which provides auxiliary data. ESA and CNES are thanked for their support of the STAFF experiment. Research at the University of Iowa was supported by the NASA Goddard Space Flight Center under Grant no. NAG5-9974. O. Santolík acknowledges additional support from Grants MSM 113200004, NSF Award no. 0307319/ME 650, and GACR 202/03/0832.

References

Anderson, R.R., Maeda, K., 1977. VLF emissions associated with enhanced magnetospheric electrons. J. Geophys. Res. 82, 135.
Baker, D.N., et al., 2002. A telescopic and microscopic view of a magnetospheric substorm on 31 march 2001. Geophys. Res. Lett. 29 (18), 1862.
Balogh, A., Carr, C.M., Acuña, M.H., Dunlop, M.W., Beek, T.J., et al., 2001. The cluster magnetic field investigation: overview of in-flight performance and initial results. Ann. Geophys. 19, 1207–1217.

Cornilleau-Wehrlin, N., Chanteur, G., Perraut, S., Rezeau, L., Robert, P., et al., 2003. First results obtained by the cluster STAFF experiment. Ann. Geophys. 21, 437–456.

Gurnett, D.A., Huff, R.L., Pickett, J.S., Persoon, A.M., Mutel, R.L., et al., 2001. First results from the cluster wideband plasma wave investigation. Ann. Geophys. 19, 1259–1272.

Helliwell, R.A., 1967. A theory of discrete emissions from the magnetosphere. J. Geophys. Res. 72, 4773–4790.

Horne, R.B., Thorne, R.M., 2003. Relativistic electron acceleration and precipitation during resonant interactions with whistler-mode chorus. Geophys. Res. Lett. 30 (10), 1527.

Inan, U.S., Platino, M., Bell, T.F., Gurnett, D.A., Pickett, J.S., 2003. Cluster measurements of rapidly moving sources of ELF/VLF chorus. J. Geophys. Res., in press.

Lauben, D.S., Inan, U.S., Bell, T.F., Kirchner, D.L., Hospodarsky, G.B., Pickett, J.S., 1998. VLF chorus emissions observed by Polar during the January 10, 1997 magnetic cloud. Geophys. Res. Lett. 25, 2995–2998.

LeDocq, M.J., Gurnett, D.A., Hospodarsky, G.B., 1998. Chorus source locations from VLF Poynting flux measurements with the Polar spacecraft. Geophys. Res. Lett. 25, 4063–4066.

Meredith, N.P., Cain, M., Horne, R.B., Thorne, R.M., Summers, D., Anderson, R.R., 2003. Evidence for chorus-driven electron acceleration to relativistic energies from a survey of geomagnetically disturbed periods. Geophys. Res. Lett. 108 (A6), 1248.

Nunn, D., Omura, Y., Matsumoto, H., Nagano, I., Yagitani, S., 1997. The numerical simulation of VLF chorus and discrete emissions observed on the Geotail satellite using a Vlasov code. J. Geophys. Res. 102 (A12), 27083–27097.

Omura, Y., Nunn, D., Matsumoto, H., Rycroft, M.J., 1991. A review of observational, theoretical and numerical studies of VLF triggered emissions. J. Atmos. Terr. Phys. 53, 351–368.

Parrot, M., Santolík, O., Cornilleau-Wehrlin, N., Maksimovic, M., Harvey, C., 2003. Source location of chorus emissions observed by Cluster. Ann. Geophys. 21 (2), 473–480.

Santolík, O., Gurnett, D.A., 2003. Transverse dimensions of chorus in the source region. Geophys. Res. Lett. 30 (2), 1031.

Santolík, O., Lefeuvre, F., Parrot, M., Rauch, J., 2001. Complete wave-vector directions of electromagnetic emissions: application to Interball-2 measurements in the nightside auroral zone. J. Geophys. Res. 106, 13191–13201.

Santolík, O., Gurnett, D.A., Pickett, J.S., Parrot, M., Cornilleau-Wehrlin, N., 2003. Spatio-temporal structure of storm-time chorus. J. Geophys. Res. 108 (A7), 1278.

Santolík, O., Gurnett, D.A., Pickett, J.S., Parrot, M., Cornilleau-Wehrlin, N., 2004. A microscopic and nanoscopic view of storm-time chorus on 31 March 2001. Geophys. Res. Lett. 31 (2), L02801.

Sazhin, S.S., Hayakawa, M., 1992. Magnetospheric chorus emissions: a review. Planet. Space Sci. 40, 681–697.

Trakhtengerts, V., 1999. A generation mechanism for chorus emission. Ann. Geophys. 17, 95–100.

Tsurutani, B.T., Smith, E.J., 1974. Postmidnight chorus: a substorm phenomenon. J. Geophys. Res. 79, 118–127.